POSTERRA

A handheld mechanism for underwater clean-up dives

Final Project Report

May 7th, 2021

University of Pennsylvania
MEAM 445/446- MEAM Senior Design
September 2020 – April 2021

Team Members

Christopher Fox
MEAM 2021
ctwfox@gmail.com

Rakesh Ravi
MEAM 2021
17ravi.rakesh@gmail.com

Hanna Kim
MEAM 2021
hmkimart@gmail.com

Seth Rogers
MEAM 2021 | ROBO 2022
sethrogersdh@gmail.com

Mona Lee
MEAM 2021 | ROBO 2021
monalee543@gmail.com

Lucille Stinn
MEAM 2021 | MEAM MSE 2022
stinn1998@gmail.com

Primary Faculty Advisor

Jennifer Lukes
Professor
University of Pennsylvania School of Engineering and Applied Sciences
Mechanical Engineering and Applied Mechanics
jrlukes@seas.upenn.edu

General Advisors

Graham Wabiszewski
Senior Lecturer
University of Pennsylvania School of Engineering and Applied Sciences
Mechanical Engineering and Applied Mechanics
grahamw@seas.upenn.edu

Adrian Armendariz
Teaching Assistant
MEAM 2020 | MEAM MSE 2021
aarmen@seas.upenn.edu

Abstract

Researchers estimate that 150 million tons by weight of plastic waste currently exists in the ocean with 8 million tons being added to this number every year [1]. Posterra is a handheld underwater device that aims to be the ultimate assistant to SCUBA divers participating in clean-up dives that target this waste. Posterra accomplishes this by allowing divers to safely remove solid waste at depths of 10 meters in the sublittoral zone of the ocean while providing a safe storage solution for the collected waste.

Posterra functions using a venturi pump optimized to maximize suction force that interfaces with a hose and mesh containment unit attached to a diver's air tank. Once a diver is underwater with Posterra, the device's suction is easily controlled by pressing a button. The venturi directs collected waste into the containment unit without threatening the diver's safety and stability underwater. An additional quick release mechanism allows the diver to remove the device in an emergency by pulling a pin on the back of the tank.

The prototype of Posterra is waterproofed to withstand prolonged submersion in saline environments with a suction velocity that increases the speed of pick up during clean-up dives by 40% and a containment unit that provides divers with a 100% increase in trash collection volume. In the future, larger scale testing that interfaces with a SCUBA diver should be performed to ensure maximum functionality, and the design should be streamlined for ease of manufacturing a product ready for consumers to purchase.

Table of Contents

I. Introduction

A. Background Information on Ocean Pollution

The world's oceans are considered to be Earth's most valuable natural resource as they make up 70% of the earth's surface and are responsible for producing over 50% of the oxygen that we breathe through the photosynthetic capabilities of phytoplankton like algae [1]. In addition to sustaining human life through this oxygen production, oceans also serve as transportation corridors, hubs for economic growth, and key sources of food for almost half of the world's population [1]. Unfortunately, pollution in the form of chemicals and solid waste threatens the vitality of Earth's most valuable natural resource, as researchers through the World Economic Forum currently estimate that at least 150 million tons by weight of plastic waste currently exists in the ocean [2, p. 7]. An additional 8 million tons are being added to the world's oceans every year with a projection that by the year 2025, the ratio of plastic to fish in the ocean by weight will be 1 ton of plastic for every 3 tons of fish, with the total weight of solid waste in the ocean surpassing the estimated weight of all ocean-inhabiting marine life by the year 2050 [2, p. 7]. A 2019 study concluded that plastic waste exists at every depth throughout the ocean with the two most common locations of settlement being coastal and shoreline regions [3]. Of the estimated 150 million tons of plastic pollution in the ocean, nearly two thirds of this plastic is considered buoyant and is concentrated in the two aforementioned regions [3]. Despite a close proximity to land, all of this waste has been shown to drift into offshore locations due to ocean currents and wind conditions where the waste can ultimately settle at deeper depths of the water column.

B. Impact of Pollution on Marine and Human Health

One of the primary concerns surrounding solid pollution is ocean acidification which closely correlates to rising ocean temperatures worldwide. Detected from a decrease in saltwater pH, acidification can be attributed to disruptions in the photosynthetic processes of phytoplankton caused by the interference of light transmission due to the accumulation of microplastics and macroplastics throughout the water column [4, p. 1]. When algae and other forms of photosynthetic plankton lose access to light caused by disruptions and pollution in the water column, these organisms cannot synthesize the high levels of carbon dioxide in the atmosphere to make food and produce the oxygen that we breathe. The resulting increase in carbon dioxide levels in the atmosphere raises the concentration of carbonic acid in the ocean and lowers the overall ocean pH towards more acidic levels. By the year 2100, at current carbon emission levels, geophysicists project that the average ocean temperature will have risen by 2°C and the ocean will have become more acidic corresponding to a drop in water pH from the current value of 8.07 to between 7.67 and 7.81 [5, p. 4]. This acidification slowly eats away at the calcium carbonate deposits in coral reefs and the shells of marine life, ultimately threatening the environments of many organisms that are crucial in the human food chain [6].

Additionally, human and marine animal health is also threatened by the increasing numbers of solid waste pollution in the ocean. When plastics enter into the ocean, many of the chemicals involved in the manufacturing processes for items such as water bottles are dissolved into the ocean or make their way into the food chain when accidentally consumed by marine animals. One element in particular that is posing health threats to both the marine environment and humans is cadmium. A common plastic stabilizer, this element is highly toxic and is classified as a carcinogen by OSHA. [7] Unfortunately, studies have recently found that the concentration of cadmium in bivalves like oysters and scallops, two shellfish species commonly consumed by humans, has been steadily increasing in parallel with ocean acidification [8]. This introduction of toxic chemicals, like cadmium, into the marine food chain is particularly impactful for humans as over 3 billion people rely on some form of seafood as the primary source of protein in their diet [9].

C. Impact of Pollution on Global Economies

It is also important to acknowledge the impact of ocean pollution on the global economy. As previously mentioned, increases in ocean acidification will have a significant impact on coral reefs and can kill these marine habitats through what is commonly referred to as bleaching. It is estimated that at the current rate of ocean acidification, a continuous two year bleaching cycle in coral reefs will be inevitable within the coming decades. This increased cyclical coral bleaching and shortening of the coral life cycle will also have devastating impacts on coastal economies that market snorkelling and SCUBA diving to tourists. In Caribbean regions like the Cayman Islands, approximately 75% of the 3.25 billion dollar (USD) gross domestic product depends on underwater tourism and commercial fishing near popular coral reefs [10, p. 26]. Continued plastic pollution in the ocean will undeniably have a dramatic effect on places like the Cayman Islands, where dying coral reefs and unhealthy marine life will not only deter tourism but also harm the fishing industry. On a larger scale, island countries and those with significant coastal regions will be similarly affected by the harm caused from plastic pollution in the oceans.

D. Solutions for Targeting Pollution

Given the knowledge that solid waste pollution in the ocean threatens both human health and economic prosperity, as well as the earth's overall climate and ecology, an investigation into existing solutions that seek to mitigate and remove plastic pollution in the ocean revealed that current technologies are limited to addressing the waste that does not sink below the water's surface. An example of current clean-up technology is exemplified in FRED, a semi-autonomous robot that utilizes conveyor belts to gather floating debris ranging in size from 10mm to 1m in size [11]. Other methods that are currently being implemented to capture trash on the ocean surface include large floating booms typically utilized in containing oil spills as well as the Seabin which functions as a floating sinkhole intended to vacuum in floating trash from harbor environments and marinas [12]. It is also worth noting that there are numerous efforts and organizations aimed at targeting solid waste pollution on beaches after trash washes to shore from the ocean. Speaking with The Ocean Project Seychelles, it was emphasized that all of the trash on the island of Aldabra washes to shore after ending up in the ocean from islands with heavy tourism nearby [13].

There are currently no forms of technology that target cleaning up plastic pollution at deeper depths of the water column. All solid waste collection efforts below the surface are limited to SCUBA divers who pick up trash by hand and carry small mesh bags during dives. Most of these dives are conducted in shoreline and coral reef environments with diving partners. The organization Dive Against Debris through Project Aware encourages divers to engage in survey clean-up dives with the goals of removing waste from the ocean and documenting the composition of debris that accumulates in specific regions. As of 2020, over 10,000 survey dives have been conducted through Project Aware with almost 2 million pieces of waste collected since the advent of the program [14]. The success of Dive Against Debris suggests that divers are aware of submerged ocean pollution and are actively involved in removing trash from the ocean floor despite the lack of technology that addresses this issue. We have designed Posterra to address the gravity of ocean pollution while leveraging the passion of SCUBA divers who participate in clean up dives.

E. Stakeholder Outreach and Interactions

To better understand the challenge of tackling a problem with such a large scope, we spoke with stakeholders who specialize in existing efforts to minimize and clean up solid waste pollution. From these interactions we became better informed of the complexities surrounding pollution clean up. One stakeholder, the inventor of Mr. Trash Wheel, notably suggested that the first step to solving a problem like ocean pollution is to spread public awareness regarding the problem and to involve as many people as possible in clean-up efforts. Increased awareness and consumer consciousness is a preventative measure that is highly effective when combined with a form of trash-collecting technology that is accessible and incentivizes removing debris from bodies of water like the ocean [15]. In order to further understand the process and efficacy of clean-up dives, a survey was distributed to an online SCUBA diving forum which collected data from 20 divers. We found that 87.5% of those surveyed had previously participated in clean-up dives with the remainder of the group willing to contribute to a clean-up dive in the future. Additionally, 56% of divers acknowledged that they felt affected by the seafloor trash even when not diving, suggesting that the emotional impacts of ocean pollution are important within the diving community. Overall, 100% of the divers surveyed said they were negatively affected when diving in trash filled areas in the ocean, suggesting that there is investment from the SCUBA community in solving this problem.

From our stakeholder interactions and research into existing solutions, Posterra was developed as a device to aid in trash removal from the ocean floor that would address the shortage in underwater solid waste collection devices. We had further in-depth conversations with divers regarding the development and design of our device and were met with enthusiasm from the SCUBA community, ultimately informing us that there is a larger demand for Posterra.

F. Social Impact of Posterra

The social impact of Posterra has been considered significantly in the design and manufacturing of our system. A fully functioning prototype of Posterra eases the experience of a clean-up dive and allows a diver to collect more trash at a faster rate than current methods. By allowing pollution to be removed from the ocean before it starts to decompose, many of the concerns surrounding carcinogens and toxic chemicals entering the food chain are limited. In a world filled with Posterra's on every diver's back, we can prevent contamination in the marine food chain from reaching the 40% of Earth's population that consumes seafood by quickly removing the sources of toxins in the environment. The benefits of Posterra on health and safety are tied closely to its impact on the environment as well. By removing macroplastics and large waste from the environment on clean-up dives, the prosperity of marine ecosystems is preserved. Dead whales will no longer wash ashore with stomachs full of man-made debris because Posterra allows divers to remove more waste from the environment before it can end up in the bellies of unsuspecting animals. Additionally, by removing pollution quickly with Posterra, the process of ocean acidification can be significantly slowed, protecting coral reefs from bleaching cycles and strengthening economies that rely on fishing and tourism attractions like snorkeling and SCUBA diving. Finally, Posterra has the potential to spread global awareness across cultures about our duty to protect our planet. The most effective solution to combating ocean pollution is prevention, yet Posterra approaches pollution with the perspective of mitigation. In a world with a fleet of Posterras roaming the ocean floors, both mitigation and prevention run parallel in promoting human health, protecting the environment, preserving economies, and uniting the world.

II. Characteristics and constraints

A. Stakeholder Needs

In-depth interviews were conducted with a variety of stakeholders, including five scuba divers, to learn the process of typical clean-up dives, the gear they use, and what they'd like to see in an additional tool. It was concluded that the final system must maintain neutral buoyancy with a total handheld weight of less than 8 pounds for the diver to be able to swim safely and smoothly. It also would have to be able to hold more than 15 gallons of trash. Furthermore, eight people in various roles at environmental nonprofits working on water clean-up efforts also informed us of different existing technologies, how plastic negatively affects coastal communities, and how we should prioritize solution characteristics. For effective use, the system should have a faster pickup rate than 1.3 lbs/hour. We also spoke with water management authority for four different bodies of water including harbors, bayous and coastal environments. Those working with inland water bodies mentioned possible restrictions due to government regulation, so the scope of Posterra was narrowed down to coastal areas. From our aforementioned survey with SCUBA divers, 20 voluntary responses informed us that 90% of divers observed trash in depths of 0-10 meters in commercial and tourist areas. With this information, the final system was designed to be usable in depths up to 10 meters underwater.

The basic template of a system that would help divers clean up trash from the sublittoral zone requires three subsystems: acquisition of trash, extension of reach, and encasement of the collected trash. All of these subsystems would have to be submersible for longer than durations of a typical dive time. The effect on the surrounding environment added constraints to ensure the safety of marine wildlife. Any exposed motor or moving part that had the potential to hurt marine animals and the environment were not incorporated into the final design. For this reason, an overhead encasement system was also eliminated in design considerations, as a floating device could confuse and disrupt the surrounding wildlife. The safety of the scuba diver was also a crucial factor. Scuba divers often carry important safety equipment strapped to their fronts, eliminating any design that would block the front of a diver, including a front-strapped bag.

The potential users of the system expressed a strong affinity towards an electric motor, as compared to a gas or diesel motor, due to the lower perceived carbon footprint of an electric motor, and stakeholders tended to be strong sustainability advocates. The electric motor also posed less risks for both the diver and surrounding wildlife in case of system failure.

B. Design Impacts of Standards

To ensure proper waterproofing, Posterra adheres to the IP and NEMA standards for waterproofing under the conditions of occasional prolonged submersion. These are standards often used in industry, and they help communicate to stakeholders the level of waterproofing our system provides, ensuring our system is up to safety standards. The Ingress Protection (IP) Rating, as defined by the international standard IEC 60529, classifies the degrees of protection provided against the intrusion of solid objects including dust, accidental contact, and water in electrical enclosures [16]. The National Electrical Manufacturer Association (NEMA) is used for electrical enclosures, and has a standard rating system that defines the enclosure's ability to withstand its environmental conditions [17]. An IP68 rating is equivalent to a NEMA 6P enclosure, which both ensure waterproofing for occasional prolonged submersion in our desired operating environment.

In addition, we utilized ASTM Designation: D870 - 15 (2020): Standard Practice for Testing Water Resistance of Coatings Using Water Immersion [18]. Since our device consists of electronic components, we needed to thoroughly test the water resistance for all components of the mechanism after they were waterproofed with a Flex-Seal or epoxy coating. The above ASTM designation outlines the standard procedure for testing submerged objects which was employed during our prototyping process. The specifications (blistering, adhesion, color loss, etc.) utilized in determining the effectiveness of our waterproofed components after they were submerged are also included in the D870 guidelines. This ASTM standard further references additional information regarding other relevant standards that were considered during the waterproofing process.

To consider diver training for stakeholders using Posterra, we used ISO 21417, a guideline for the implementation of environmental and ecological awareness education in recreational diver training [19]. This standard was relevant to our project as we considered what underwater practices divers are already being taught to reduce the environmental impact of divers.

As targeting the appropriate ocean trash was a key driver in our engineering, we looked at ASTM D5231 - 92 [20]. This standard considers the composition of municipal solid waste to determine various patterns in a specific geographical area. This allows planners to change processes involved with solid waste collection and waste management facilities. It gives us an understanding of the makeup of solid waste to be used to push for legislation that can put bans on specific types of solid waste that may be troublesome to remove from the environment, such as plastic bags and styrofoam containers. This standard was important when looking at the makeup of solid waste that ends up in the oceans and helped us engineer a device that effectively targets the most common types of waste.

As we selected a 12-volt electric bilge pump in our final prototype, we looked at code ABYC H-22: DC Electric Bilge Pumps Operating under 50 Volts [21]. These standards were used to guide the installation and operation of the electric bilge pump we purchased off the shelf and incorporated into our design to make sure that the pump was used without interference and safety issues.

III. Design, engineering, and realization

A. Acquisition

A minimum flow rate must be achievable by the system in order to efficiently pull objects into an encasement. For objects in water, this depends on the velocity at the inlet of the tube used to pull objects into Posterra's encasement (Appendix A-1). The data for the required inlet velocity for a variety of objects is summarized in Table I below.

TABLE I: Required Flow for Common Seafloor Trash in 3" Diameter Tubing

Object	Max Area (10^{-3} m^2)	Mass (10^{-3} kg)	Inlet Velocity (m/s)	Inlet Flow Rate (GPH)
12oz Can	6	15	0.23	976
Plastic Bag	50	0.4	0.01	45
Cigarette Butts	0.24	0.17	0.12	512
Snickers Wrapper	12	0.32	0.016	69
Bottle Caps	7	2	0.06	273
Straws	1.2	0.4	0.08	351
20oz Pepsi Bottle	16	2.4	0.17	744
16oz Plastic Cup	6	5	0.12	546
12oz Glass Bottle	17	190	0.47	2024
Sand	0.00078	0.0044	0.33	1444

Since the above flow velocities refer to those at the very end of the system, it was imperative to maximize efficiency and minimize head losses from friction and turbidity in the hose connected components.

1) Pump:

After subsystem downselection, the team determined that an electric pump would be the ideal option to drive the flow throughout our system. A low voltage (<60V) pump was determined to be the best option since high voltage battery configurations would not be a viable option due to weight and space constraints. We also aimed to minimize electronic complexity as well as power losses when changing voltage levels. It is rare for low voltage pumps to generally move the flow rate of water required by Posterra, since these systems are generally stationary and connected to high voltage electrical outlets. An in depth search of various pumps found that a number of centrifugal pumps and certain varieties of positive displacement pumps, such as diaphragm pumps and peristaltic pumps were the main options for low voltage pumps, but few met Posterra's flow requirements and were in an adequate price range. Positive displacement pumps do not suffer substantial losses to flow rate when pumping at an increased head, but are generally utilized for lower flow rate applications. Centrifugal style bilge pumps, which do suffer substantial flow rate losses at increased head, were the only low voltage pumps that greatly exceeded our estimated flow rate requirement of over 2000 gallons per hour (GPH).

Bilge pumps are traditionally made to connect to the batteries of aquatic vehicles, and for this reason are traditionally offered in 12V and 24V varieties. They are offered in flow rates ranging from around 300 GPH up to 8000 GPH. Initially, it seemed as if Posterra would be easily powered with a 4700GPH pump by Seaflo (technical specifications in the Appendix A-2). While it was difficult to determine the true head losses by our system, initial simulations showed that a flow rate of approximately 4000 GPH from the pump would be adequate to achieve 0.46 m/s flow at the inlet. Following empirical testing, it was determined that Posterra's venturi system would see considerable effective head losses, and that the flow curve published by the pump's manufacturer was not accurate to the calculated effective head even in testing conditions with constant diameter tubing. Almost double the expected flow rate would be required to achieve our inlet suction, so Xylem's Rule Evacuator 8000 was chosen to generate fluid flow as it is the only low voltage pump on the market that achieves a flow rate of over 6000 GPH [29].

2) Venturi:

Since the pump cannot safely intake trash and other particulates, Posterra employs the use of a venturi junction to transport the trash in a safe yet effective manner. A common venturi junction features three sections: a nozzle where the area of the tube decreases and fluid velocity increases, a channel where the fluid velocity is steady in the narrow portion of the tube, and a diffuser where the area of the tube increases and fluid velocity decreases. A venturi injector is a device that induces a suction flow by attaching an inlet tube to the venturi channel, which served as the basis for our design. Venturi injectors produce a secondary flow solely through the use of pressure gradients. Bernoulli's principle shows that the pressure of the fluid in the channel is lower than the pressure of the fluid in the nozzle and diffuser. This low pressure region induces a suction flow in the inlet tube as the pressure in the channel is lower than the environmental pressure. However, in order for this to work, the suction tube must have the same or smaller diameter than the venturi channel, which was not attainable for our use case. A sample venturi geometry has been included below in Figure 1.

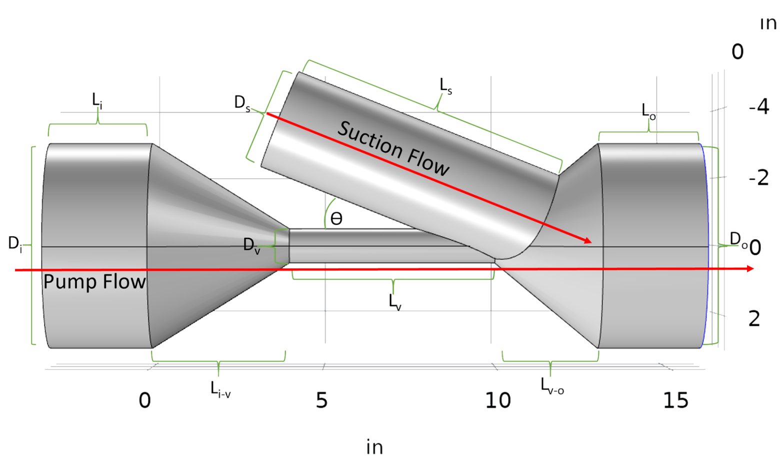

Figure 1: Example of Venturi Junction Showing Flow

Posterra requires a suction tube diameter of 3" in order to accommodate the full range of seafloor trash that is being targeted, so the venturi channel would need to be greater than 3" in diameter. Since the outlet of the pump was also 3" in diameter, there would effectively be no change in pressure, resulting in minimal suction. In order to design a suction inlet that would fit Posterra's needs, a ComSol model of a standard venturi junction was built to analyze the pressure dynamics of the system. Through this initial modeling it was found that as the angle of the diffuser increases, an additional low pressure region is found along the walls of the diffuser. Moreover, as the exit velocity from the venturi channel increases, a central jet in the diffuser and outlet sections becomes more prominent. These two findings became integral to the design of Posterra's venturi junction.

Since venturi injectors have proven that low pressure gradients are a viable method of producing a suction flow, Posterra's venturi design process first focused on optimizing the suction inlet placement based on the simulated pressure gradients. This resulted in the suction inlet being placed on the diffuser wall to maximize the contact area with the low pressure region.

The addition of the suction inlet inherently changes the fluid dynamics, combinations of diffuser lengths, outlet diameters, outlet lengths, and suction inlet angles were all tested in order to maximize the simulated suction flow rate. In all the conducted simulations, the flow rate into the venturi was 4000 GPH while the outlet and suction inlet were both set as open boundaries at 0 gage pressure to ensure that the model closely reflected Posterra's operating conditions. Through these initial sets of simulations, optimal ranges for the listed key design parameters were found. The optimal inlet angle was between 0.4 and 0.5 radians, the optimal channel diameter was 0.6 to 0.8 inches, the optimal outlet diameter was between 4.5 and 5 inches, and the optimal outlet length was between 2.5 and 4 inches. In these ranges of optimal configurations, the simulated suction velocity peaked at 1.1m/s and a sample of the fluid dynamic simulation can be seen below in Figure 2. (It is important to note that small variations in geometry can have large impacts on the suction velocity, so the maximum attainable velocity in this range of parameters can be higher. However, 1.1m/s is the maximum of all tested configurations.)

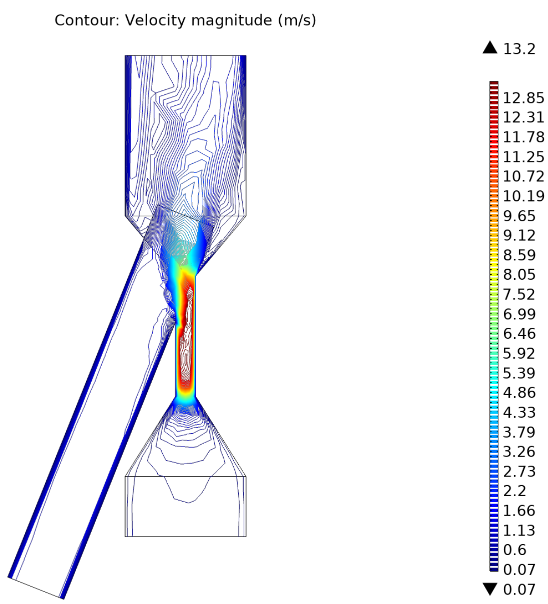

Figure 2: COMSOL Simulation Results

In order to increase the suction flow velocity of the system, geometries that induced entrainment were also analyzed. Entrainment is a physics phenomenon that often occurs in jetted environments. When a jet of fluid travels through a medium, turbulence occurs at the jet-medium boundary. This turbulent layer acts as a mixing tool, pulling the outer medium closer to the jet stream. When the medium and the jet come into contact the shear forces acting on the medium pull it into the jet stream. Utilizing this principle, the venturi channel was extended into the diffuser section to produce a jet stream in the center of the outlet. As the exit of the venturi channel is within the suction tube, the jet stream is able to augment the suction velocity via entrainment. With the addition of jetting, the simulated suction velocity increased from 1.1m/s to 2.8 m/s. However, the models showed a reversed flow direction towards the edges of the venturi outlet on account of the large turbulent region created by the jet stream. On account of this, simulations were performed with various channel extension lengths to balance the suction velocity increase with the size of the turbulent region as shown in Figure 3. The geometry that provided this balance produced a suction velocity of 1.45m/s without inducing backflow.

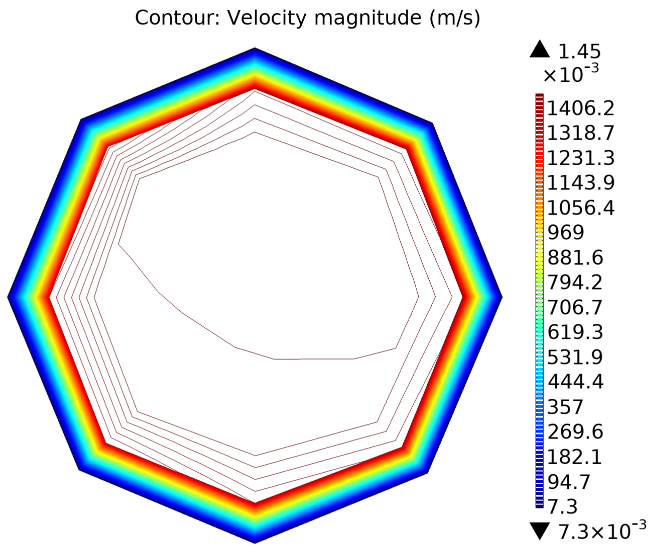

Figure 3: Results from Channel Extension Simulation

3) 3D Printing and Testing:

To help validate the CFD results and determine real world losses, it was necessary to perform tests using various venturi geometries along with the bilge pump. Multiple complex venturi geometries needed to be quickly and cheaply manufactured, so the team set out to 3D print a variety of venturi geometries using Ender 3 Pro fused deposition modeling (FDM) printers. Over the course of approximately two months, 9 various geometries that showed promise during simulations were printed and tested (see Appendix A-3). In addition to changing the geometry of the prints, various methods were also utilized in an attempt to minimize losses by achieving the smoothest surface finish on the inside of the venturi tubes: printing separate halves to minimize overhang, printing in different orientations, and lining the insides of poor quality prints with sealers such as Flex Seal (thinned with acetone), Polyurethane, and Polyacrylic. Unfortunately, a myriad of 3D printer issues plagued two of the team's 3D printers, and quality between prints varied greatly, and it was difficult to empirically determine the efficiencies of different venturi geometries. The best performing simulation geometry performed marginally better than other geometries, and a slightly extended version was printed in a clear SLA material for the final prototype. In contrast to the FDM prints, the SLA print had a very smooth interior and was non-porous. As expected, this venturi outperformed all of the previous prints, and was used in determining the actual flow rate of our system. Due to price constraints, the team could unfortunately not print all the earlier prints in the same material, which would surely have simplified testing and allowed for much more robust results.

B. Extension

To determine the optimal tubing and length for our extension subsystem, quantitative downselection was performed for hoses with varying characteristics and flow testing was performed to determine the optimal length. Five hose options were evaluated based on bend radius, interior surface texture, maximum pressure, operating conditions, and cost. For the extension subsystem to operate around a diver's body, the average male waist circumference [22] was used to calculate a maximum allowable bend radius of eight inches. In order to minimize head losses from friction through the tubing, a smooth interior surface texture would perform better than a corrugated interior surface texture. With intended operation in liquids and the pump calculations, the maximum pressure within the pump should not exceed 0.5 psi at a 10 meter depth in ocean water. Based on these system characteristics, two hoses intended for use with liquids, one more flexible and one less flexible, were tested to determine impacts of friction on flow rate.

Both hoses were tested at their full length of 9 feet and the more flexible hose was tested at a shorter length of 5 feet (Appendix A-4). Each flow test consisted of connecting the hose to the bilge pump within the testing pool, elevating the free end of the hose out of the water to a designated height outside of the pool and above a basin, running the pump until the basin was full, and measuring the time to fill and amount of water passed through the system. This test assessed the flow rate through the pump and hoses as well as was used to calculate the head losses due to friction in order to determine the final hose option. The collected data, shown in Figure 4, demonstrated relatively small head losses due to friction at these lengths and a greater flow rate with shorter hose lengths. With similar performances for both hoses, the flexible hose was chosen for easier usability and its lighter mass. Also with a target flow rate, the length of the hose was maximized for maximum offered extension and a hose length of 3 feet 7 inches was determined.

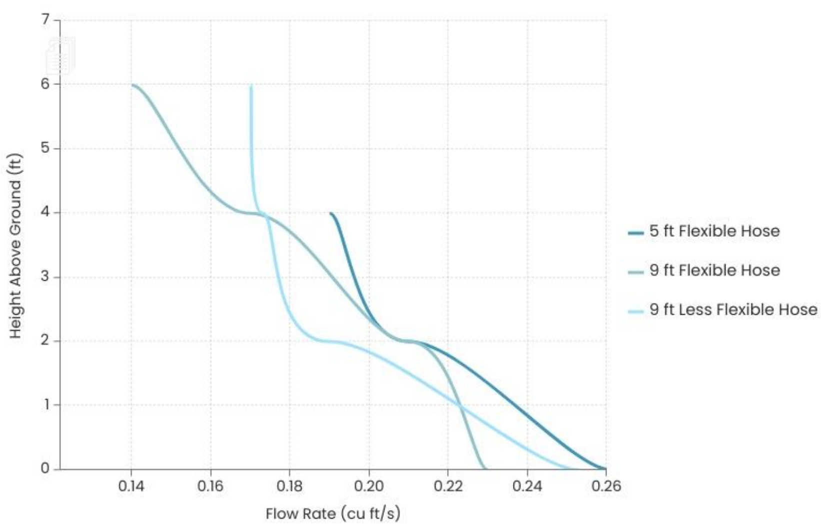

Figure 4: Results of Hose Testing

C. Encasement

The encasement subsystem holds the trash after it has been sucked in by the diver. It consists of the aluminum base plate at the bottom, to which all other components are rigidly connected, as well as a tapered enclosure constructed of aluminum extruded mesh panels. Both the baseplate and mesh have many small openings to minimize the additional effort that a diver must exert while using Posterra. This way, water or air do not get trapped in enclosed cavities, the drag forces on a swimming diver are greatly reduced, and weight is minimized. Additionally, small animals such as crabs, fish, and seahorses that may be transferred into the encasement via the hose can escape through the mesh or the 50 small cutouts in the baseplate. The materials for the encasement, 6061 aluminum for the baseplate and 3003 aluminum for the mesh were chosen due to their resistance to corrosion, low weight, and ease of manufacturability. Both materials were also chosen in thicknesses where only negligible deflections would be present in expected load cases. Rigidity is important for the encasement, because it does not allow for the encasement to get tangled easily, and will not move around and cause difficulties for the diver as they attempt to swim or pick up trash. Expanded aluminum mesh proved to be the ideal option for the body of the encasement as the light rigidity of the extruded aluminum mesh, along with it's much greater resistance to getting cut open and getting tangled, made it the ideal option for the body of the encasement when compared to screens or netting.

D. Electronics and Battery

A 12 V 10 Ah capacity nickel metal hydride (NiMH) battery was identified as the optimal power source for Posterra given that it is protected against thermal runaway with an ability to operate reliably in environments between -5 and 95 degrees Fahrenheit, as well as high energy capacity and ideal deep-discharge qualities. Our team initially considered other types of batteries to power the system including lithium-ion (Li) and lithium iron phosphate ($LiFePO_4$). However, an extensive down selection process informed us that an NiMH battery was ultimately the safest and most efficient option for Posterra. Moreover, this particular down selection process evaluated the specific energy, capacity, maximum voltage, discharging ability, and life cycle associated with each battery. Table II below summarizes the metrics that informed the down selection process, as well as individual ratings for each battery that was considered.

TABLE II: Downselection Summary of Battery Types

Battery Type	Lithium-Ion [23]	$LiFePO_4$ [24]	NiMH [25]
Specific Energy (Wh/kg)	150 - 200	90-120	70-100
Overall Safety	**B-**: Highly reactive but capable of withstanding a wide range of temperatures.	**B+**: Moderately reactive, however exhibits thermal and chemical stability and mInimal degradation at high temperatures.	**A**: Minimally reactive, however, extreme temperatures will result in a drop in voltage output
Capacity (mAH)	1500	1100	2200
Max Voltage per Cell (V)	3.7	4.2	1.2
Discharging Ability	Not fully dischargeable	Not fully dischargeable	Fully dischargeable
Life Cycle	500-1000	1000-10000	180-2000

1) Battery Chemistry:

In a nickel metal hydride battery, the positive electrode is nickel oxyhydroxide NiOOH and the negative electrode is hydrogen storage alloy M. During charging and discharging, OH– ions migrate between the electrodes. Since nickel hydride batteries use an aqueous solution of potassium KOH as the electrolyte, oxygen is produced at the positive electrode at the end of charging due to electrolysis of OH– . This oxygen reaches the negative electrode and reacts with water, and thus is reconverted to OH–. Below in Figure 5 is a schematic of the electrochemical reaction that occurs inside the battery.

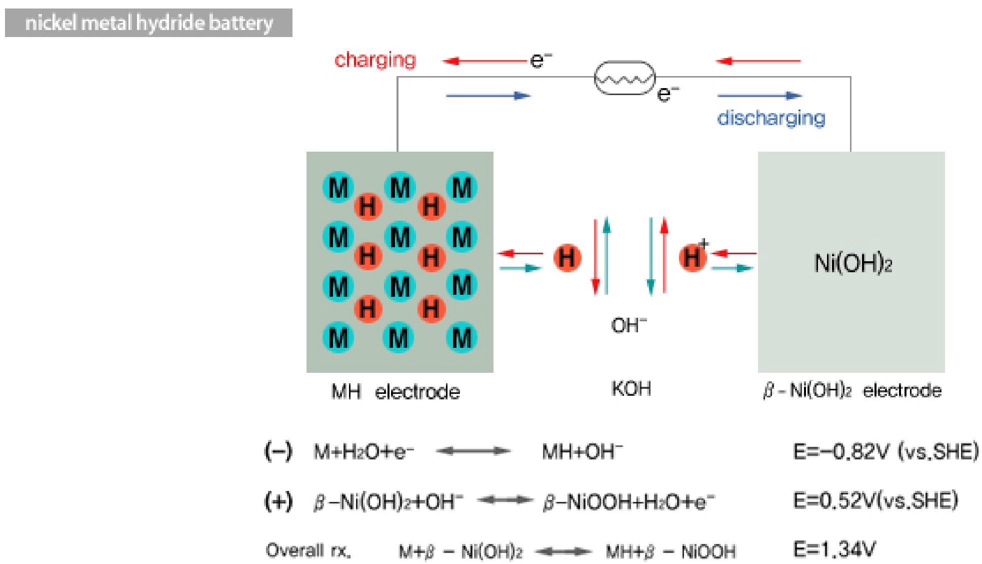

FIGURE 5: Schematic of Nickel-Metal Hydride Battery Chemistry

2) Battery Performance:

The heat generated by the battery during charging and discharging primarily due to the battery's resistance and overpotential. The rate of change of the battery's temperature is proportional to the total heat that the battery generates minus the heat that the battery loses to its surroundings. The waterproof enclosure for the battery facilitates heat transfer primarily via conduction through an aluminum housing to the marine environment. Internal resistance and voltage testing was performed in order to identify the amount of heat generated by the battery which is approximately 81.12 W. Moreover, we found that the pump draws 26 amps from the battery when attached to the venturi and the flex hose. At this discharge rate the battery will reach a cutoff voltage of 9 V in approximately 18 minutes.

The geometry of the battery was chosen such that it would fit inside a NEMA 6P enclosure with the additional space for its leads to connect to the bilge pump. Additionally, its voltage and capacity were optimized such that the battery could accomodate a 20% duty cycle for a 85 minute dive (which is approximately 17 minutes). This particular nickel metal hydride battery will last between 500 - 1000 cycles and the full metrics are described in Table III.

TABLE III: Full NiMH Battery Metrics

Battery Type	Nickel Metal Hydride (NiMH)
Given Battery Specs	12 V, 10 Ah, 10 30A D cells (2x5 assembly)
Voltage	12 V (working), 14.5 V (peak)
Capacity	10 Ah/120 wh
Charging Rate	1.8 A (standard), 5 A (max) for each 12 V 10 Ah module
Discharging Rate	10 A (standard), 20 A (continuous max), 30 A (max)
Dimension (LxWxH)	6.5" (165 mm) x 2.64" (67 mm) x 2.64" (67 mm)
Battery Weight	3.6 lbs (1650 g)

3) Battery Modeling:

A Simulink model was used in order to approximate the current draw from the battery using a series of pump, venturi, and hose assemblies. In particular, the model allowed for the actual discharge curve of the battery, built from testing data, to be mapped to a hypothetical discharge curve associated with variable current draws shown in Figure 6. For acute venturi geometries with larger pressure gradients, and extended hose lengths, the pump drew a current of approximately 26 Amps. Without the venturi or hose attached, the current draw was approximately 17 Amps.

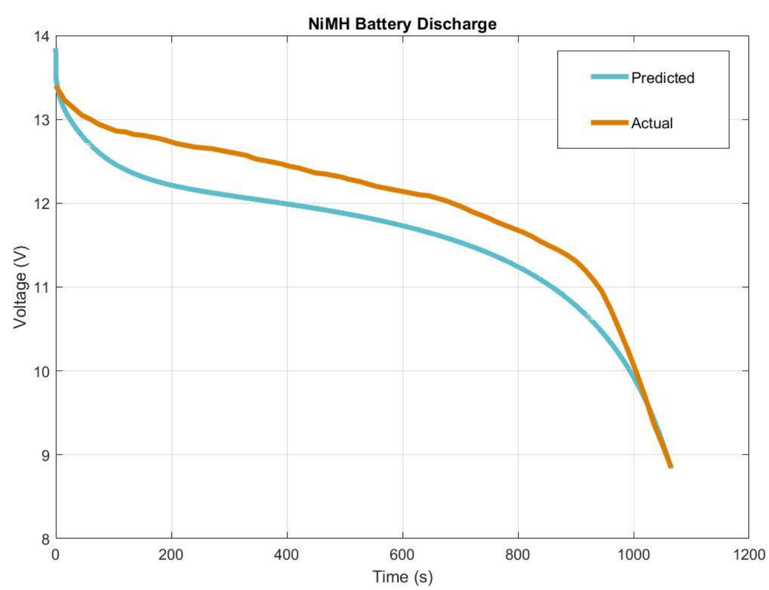

Figure 6: Simulink Simulation Results for Battery Discharge

In the simulation, the NiMH battery is connected to a constant load of 26 Amps. A DC machine is connected in parallel with the load and operates at no load torque. When the State-Of-Charge

(SOC) of the battery goes under 0.05 (5%), a negative load torque of 200 Nm is applied to the machine such that it acts as a generator to recharge the battery. When the SOC goes over 80%, the load torque is removed so only the battery supplies the 26 Amps load. The battery voltage, SOC, motor speed and motor current signals are available at the output of the block.

At t = 0 s, the DC machine is started with the battery power. The speed increases to 120 rad/s. The battery is also discharged by the constant DC load of 26 amps. At t = 1150 s, the SOC drops under 5%. A mechanical torque of -200 Nm is applied to the machine so it acts as a generator and provides a current of 26 amps. Hence, 13 amps goes to the load and 13 amps goes to recharge the battery. At t = 1470 s, the SOC goes over 80%. The mechanical torque is removed and the machine operates free. Then the cycle restarts (see full model in Appendix A-5)

E. Safety

From a safety perspective, the team prioritized the diver's safety while using Posterra, which drove the addition of a quick release mechanism to ensure that the diver is capable of removing the entire device by pulling out two quick release pins in the event of emergency. Given the electronic nature of our system as well, the type of battery and the complete waterproofing of all electronics was required during testing and assembly. This was to ensure that the diver would be safe from the 12 V power supply that was implemented in the design.

A waterproof and tear resistant conduit contains the wiring harness to connect the pump to the battery, which is housed in a NEMA 6P rated aluminum enclosure- the highest rating that allows for "occasional prolonged submersion". The enclosure is made from die-cast aluminum and is resistant to rust, corrosion, and abrasion. The enclosure also integrates a ½" diameter conduit for wiring waterproof fittings as well. The full electronics and enclosure assembly for Posterra was waterproofed and successfully tested at a depth of 3 feet. The on/off switch is also rated to an IP68 standard and was given an additional flex seal coating. All critical subsystems of Posterra were tested to withstand 24 hours of continuous submersion as well.

On a larger scale, acknowledging the threat of certain plastics in releasing additional chemicals, like cadmium, into the environment, we made sure that our prototype did not incorporate any plastics that had been stabilized by carcinogens and we also chose aluminum over steel to prevent rust on exterior subsystems that had sharper geometries with the potential to come into contact with human skin. Ideally, a consumer version of Posterra would utilize recycled materials that appeal to our environmentally conscious customer base.

IV. Final System Form

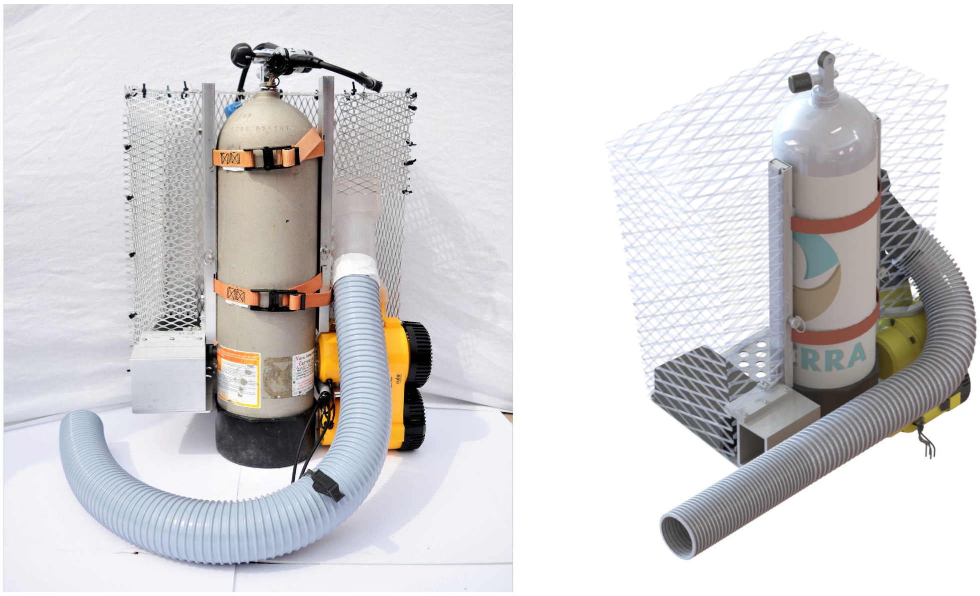

Figure 7: Final System Form

The final prototype of the system is shown in Figure 7. Table IV below has the final performance metrics for the system form compared to the original core objectives for the project.

TABLE IV: Final performance metrics

Metric	Goal	Reality
Useable depth	10 meters	10 meters
Handheld weight	< 8 lbs	3.2 lbs
Volume of trash	15 gallons	14.5 gallons
Rate of pickup	> 1.3 lbs/hr	Undetermined

The final encasement performed under the target characteristic for volume of trash held because the final constructed encasement followed a rectangular geometry instead of a trapezoidal geometry due to construction constraints. These dimensions would be altered for future developments of this project. The final system form was not able to be tested for rate of pickup due to limitations in testing environments.

Discussing Posterra's impact, in coral environments, divers no longer need another person to hold a collection bag because Posterra is hands-free resulting in a 100% increase in trash collection ability. A larger capacity for the encasement eliminates the need to resurface during a dive and increases the length of dives by 10 minutes resulting in a 12% increase in dive durations. Increased collection speed also saves an estimated 7 minutes that can be added to the total dive time, resulting in 40% faster trash collection.

V. System performance

While the team was fortunate enough to build a full prototype of Posterra, full diver testing was unattainable due to Covid-19 restrictions on the campus pool. However, flow rate testing with the SLA printed venturi and 3'7" hose was performed in a kiddie pool, achieving a flow rate of approximately 0.23 m/s, and a flow rate of 0.7 m/s without the hose. This flow is exactly half of the desired flow rate of 0.46 m/s, and is only strong enough to pull small objects such as bottle caps, plastic lids, plastic straws and stirrers, and cigarette butts. While we were unable to reach our goal of larger objects, these 4 groups of aforementioned objects are all in the top ten of the most commonly found objects on cleanup dives. All together, these objects make up just over 22% of the total items found during cleanup dives, according to a study by the The Ocean Conservancy released in their 2018 yearly report [26].

Although the experimental flow rates did not match the simulated values, the tests conducted gave valuable insight into the effects that trash objects had on the suction flow. Since the velocity gradient in the suction tube is asymmetric, objects that entered the suction tube quickly began to tumble. This reduced the speed at which the trash could travel as well as made the flow inside the suction tube more turbulent. Additionally, this increased turbulence persisted when the trash entered the outlet of the venturi junction. The turbulence along the edges of the outlet caused light objects to stagnate as they attempted to exit the junction. This turbulence and asymmetry was also evidenced in dye tests that were performed as dye that was deposited in different spots along the suction inlet would enter the jetstream with skewed probabilities. This information is essential in designing a more efficient venturi junction and also suggests that slightly higher flow velocities may be required to reduce the effects of the asymmetric velocity gradient.

VI. Conclusions and Future Work

As mentioned in the previous section, we were significantly limited in our ability to prototype and test our system due to the constraints of the time. Overall though, we were able to achieve a successful prototype of our system that was tested at the depth of 3 feet in a kiddie pool with full waterproof functionality. In analyzing the efficacy of Posterra, future work with the system would require us to test our device on a larger scale in a body of water that would allow a SCUBA diver to fully interact with the system. Notably, we were unable to acquire a buoyancy control device that could be used during diving which would have allowed us to achieve a larger scale of testing.

Furthermore, for Posterra to become a more efficient and viable solution for ocean floor cleanup, the suction power needs to be increased. This would allow Posterra to pick up a wider array of objects including glass bottles and aluminum cans, and pick up lighter objects with reduced time. Additional ComSol simulations suggest that higher suction velocities are capable with different venturi junction geometries. The size and geometry of the junctions analyzed were restricted to the capabilities of the Creality Ender 3 Pro. The simulations have shown that by increasing the overall length of the junction, higher suction velocities can be achieved without inducing backflow. Additionally, the length restrictions resulted in a very steep nozzle design. On account of this, the walls of the nozzle experience high fluid pressure, increasing the effective head of the junction. With a longer nozzle as shown in Figure 8, the effective head of the junction can be reduced which would allow the pump to push water into the junction at a higher flow rate. With these changes, Posterra could achieve a suction flow velocity of up to 4.45m/s using the same bilge pump.

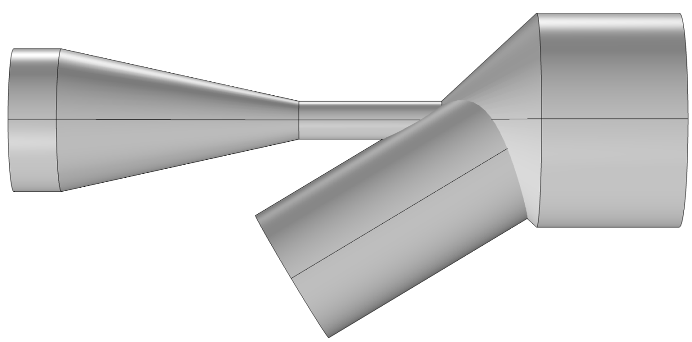

Figure 8: Future Venturi Geometry for Higher Flow Rate

It is very likely that with more time and resources the flow rate of our system could be doubled to achieve our ideal flow. A smoother hose, further optimized venturi, and a pump specifically designed for this application would all help to achieve this goal, and these aforementioned aspects of Posterra would be the focus of any future work.

VII. Statement of Roles

Christopher Fox

Chris was primarily involved with pump selection, manufacturer outreach, and creating a CAD model of our system with design for manufacturing and design for assembly in mind. Chris also put forth a significant amount of effort in material selection, finalizing the hose selection, and participating in the venturi testing. Chris was heavily involved in the fabrication of Posterra emphasizing 3D printing, machining, fabricating the wiring harness, and the waterproofing of the system.

Hanna Kim

Hanna was responsible for design sketches and system visualization throughout the process. She also drove the subsystem allocation and the quantitative downselection for each subsystem. She filed and submitted the financial forms for appropriate reimbursement and spending of budget. She assisted in the CAD model finalization, and she contributed to the fabrication and assembly of the final Posterra prototype.

Mona Lee

Mona managed stakeholder outreach and oversaw the creation of all presentation materials. Mona also contributed to hose and venturi testing, performing the calculations to downselect tubing and calculate extension length. Mona also aided in the encasement and overall system construction.

Rakesh Ravi

Rakesh was primarily responsible for the team's venturi junction design and for performing computational fluid dynamics on our system. Rakesh also contributed to 3D printing and the venturi testing. Rakesh was also involved in the assembly of the final Posterra prototype.

Seth Rogers

Seth was primarily responsible for identifying an appropriate power source for Posterra through various down selection processes. Moreover, Seth was responsible for integrating the battery subsystem into the final assembly. This involved battery SOC and internal resistance testing in conjunction with pump/venturi/hose geometry testing as well. Seth also assisted with assembling the final Posterra prototype.

Lucille Stinn

Lucy was the primary project manager for Posterra and was responsible for making sure assignments were completed on time and the team was conscious of deadlines. Lucy also contributed to venturi testing, waterproof testing, and consolidating background information on the project. Lucy was heavily involved in purchasing, machining and manufacturing, and the project's documentation/presentations.

VIII. Acknowledgements

We would like to extend our deepest appreciation and gratitude to the following people who allowed us to achieve our goals with Posterra!

Paul Campagna
Market Application Manager at Xylem Inc.
Consultant for commercial pump market, performance, and testing; provided technical documents and CAD for the pump; Donated the Rule Evacuator 8000 on behalf of Xylem.

Pete Szczesniak
Manager, Manufacturing and Fabrication Services at Penn
Manufacturing Consultant

Peter Bruno
Educational Laboratory Coordinator
Manufacturing Consultant, AddLab Coordinator

Jason Pastor
Instrumentation Technician at Penn
Manufacturing Consultant

Joe Valdez
Instrumentation Technician
Manufacturing Consultant

Alan Nunez
MEAM '21
AddLab Staff and Venturi Manufacturing

Justin Duhamel
MEAM '22
Wiring Harness Technical Consultant

Dina Marble
Founder of Family Dive Club
Key Stakeholder and SCUBA Diving Consultant

Foster Collins
Mechanical Engineer at Sarcos and former member of SCUBAssist
Waterproofing and Senior Design Consultant

References

[1] US Department of Commerce, National Oceanic and Atmospheric Administration, "Why should we care about the ocean?," 2017.

[2] World Economic Forum, "The New Plastics Economy: Rethinking the Future of Plastics," Jan. 2016.

[3] Lebreton, L., Egger, M. & Slat, B., "A global mass budget for positively buoyant macroplastic debris in the ocean," *Sci Rep* 9, 12922 (2019). https://doi.org/10.1038/s41598-019-49413-5

[4] M. Shen et al., "Can microplastics pose a threat to ocean carbon sequestration?," Mar. Pollut. Bull., vol. 150, no. 110712, p. 110712, 2020.

[5] D. Bernie, J. Lowe, T. Tyrrell, and O. Legge, "Influence of mitigation policy on ocean acidification: Mitigation of Ocean Acidification," Geophys. Res. Lett., vol. 37, no. 15, 2010.

[6] J. Silverman, B. Lazar, L. Cao, K. Caldeira, and J. Erez, "Coral reefs may start dissolving when atmospheric CO2 doubles," Geophys. Res. Lett., vol. 36, no. 5, 2009.

[7] "Cadmium Standards," *1926.1127 - Cadmium | Occupational Safety and Health Administration*. [Online]. Available: https://www.osha.gov/laws-regs/regulations/standardnumber/1926/1926.1127. [Accessed: 07-May-2021].

[8] W. Shi, X. Zhao, Y. Han, Z. Che, X. Chai, and G. Liu, "Ocean acidification increases cadmium accumulation in marine bivalves: a potential threat to seafood safety," Sci. Rep., vol. 6, no. 1, p. 20197, 2016.

[9] "Sustainable Seafood," *WWF*. [Online]. Available: https://www.worldwildlife.org/industries/sustainable-seafood#:~:text=Approximately%203%20billion%20people%20in,to%20billions%20of%20people%20worldwide. [Accessed: 07-May-2021].

[10] UK Government Office for Science, "Foresight Future of the Sea: final report," Mar. 2018.

[11] "Meet Fred – clear blue sea," Clearbluesea.org. [Online]. Available: https://www.clearbluesea.org/meet-fred/. [Accessed: 16-Nov-2020].

[12] "The Seabin V5 – the Seabin project - for cleaner oceans," Seabinproject.com, 17-Jan-2019. [Online]. Available: https://seabinproject.com/the-seabin-v5/. [Accessed: 16-Nov-2020].

[13] J. Raguain, 06-Oct-2020.

[14] "Dive against debris® map," Projectaware.org. [Online]. Available: https://www.projectaware.org/diveagainstdebrismap. [Accessed: 16-Nov-2020].

[15] J. Kellett, 23-Oct-2020.

[16] "IP Rating Chart," *DSMT.com*. [Online]. Available: http://www.dsmt.com/resources/ip-rating-chart/. [Accessed: 05-May-2021].

[17] "NEMA Enclosure Ratings," *Nema Enclosures*. [Online]. Available: https://www.nemaenclosures.com/enclosure-ratings/nema-rated-enclosures.html. [Accessed: 05-May-2021].

[18] Standard Practice for Testing Water Resistance of Coatings Using Water Immersion, ASTM D870 - 15, 2020.

[19] "ISO 21417," *ISO*. [Online]. Available: https://www.iso.org/obp/ui/#iso:std:iso:21417:ed-1:v1:en. [Accessed: 05-May-2021].

[20] Standard Test Method for Determination of the Composition of Unprocessed Municipal Solid Waste, ASTM D870 - 15, 2003.

[21] DC Electric Bilge Pumps Operating Under 50 Volts, ABYC H-22, 1986.

[22] "FastStats - Body Measurements," *Centers for Disease Control and Prevention*, 14-Jan-2021. [Online]. Available:

https://www.cdc.gov/nchs/fastats/body-measurements.htm?fbclid=IwAR2Lkt8JEIyT72p1YX7QUb8l2yjyLwBJ-6xeoWBYO5KQ8VEjwIit6INW8IU. [Accessed: 05-May-2021].

[23] "Lithium 18650 Rechargeable Cell," batteryspace.com. [Online]. Available: https://www.batteryspace.com/samsung-lithium-18650-rechargeable-cell-3-7v-1500mah-5-55wh-23a-rate---inr18650-15m---un-38-3-passed.aspx [Accessed: 1-March-2021].

[24] "A123 LiFePO4 26650 Rechargeable Cell," batteryspace.com. [Online]. Available: https://www.batteryspace.com/a123-lifepo4-26650-rechargeable-cell-3-3v-2500-mah-50a-rate-8-25wh-anr26650m1b---un38-3-passed-and-iec-listed.aspx. [Accessed: 8-Dec-2020].

[25] "NiMH Battery Pack: 12V 10Ah (120 Wh 2x5D) for Portable Devices," batteryspace.com. [Online]. Available: https://www.batteryspace.com/nimh-battery-pack-12v-10ah-120-wh-2x5d-for-portable-devices.aspx [Accessed: 10-Feb-2021].

[26] *Building a Clean Swell*, Ocean Conservancy Cleanup Reports, June 2018. [Online]. Available: https://oceanconservancy.org/wp-content/uploads/2018/06/FINAL-2018-ICC-REPORT.pdf

[27] "SEAFLO 01 Series 4700GPH Seaflo Bilge Pump," *Small Boat Bilge Pump | SEAFLO 3500 GPH 12v Submersible Marine Electric Bilge Pump*. [Online]. Available: http://www.seaflo.com/en-us/product/detail/623.html. [Accessed: 07-May-2021].

[28] "Plug-In Utility Pump, Body Material Acetal, Max. Head 22.0 ft", grainger.com. [Online] Available: https://www.grainger.com/product/6PWA8?ef_id=EAIaIQobChMI2c3Kjt2U7wIVwfDjBx3q_Q5EEAQYASABEgKoNPD_BwE%3AG%3As&s_kwcid=AL!2966!3!281698275978!!!g!469894314406!&gucid=N%3AN%3APS%3APaid%3AGGL%3ACSM-2295%3A4P7A1P%3A20501231&gclid=EAIaIQobChMI2c3Kjt2U7wIVwfDjBx3q_Q5EEAQYASABEgKoNPD_BwE&gclsrc=aw.ds&fbclid=IwAR3bRDQ3Q4m9VhJ4_JLHp82tPleaD111Ka9IwvDmrxhetemxbpcGZpZjFrE [Accessed: 10-Jan-2021].

Appendix

A-1: Flow Analysis for Most Common Types of Ocean Pollution

Type	Max Area	Mass	Cf	F	Velocity	Pipe D	Flow Rate	Mass Flow Ratio (%)
12oz Can	0.00582	0.015	1	0.14715	0.225209	5	2711.713	57.69601
Plastic Bag	0.05	0.0003884	1.4	0.00381	0.010449	5	125.8201	2.677024
Cigarette Butts	0.00024	0.00017	1	0.001668	0.118065	5	1421.603	30.24688
Snickers Wrapper	0.0123	0.00032	2	0.003139	0.016	5	192.6491	4.098917
Bottle Caps	0.007065	0.002	1.4	0.01962	0.063081	5	759.5466	16.16057
Straws	0.0012	0.0004	1	0.003924	0.080992	5	975.2117	20.74919
20oz pepsi bottle	0.0159	0.02383	1	0.233772	0.171738	5	2067.869	43.99721
16 oz Plastic Cup	0.006206	0.005	1	0.04905	0.125916	5	1516.138	32.25825
12oz glass bottle	0.01715	0.19	1	1.8639	0.466924	5	5622.174	119.6207

Type	Max Area	Mass	Cf	F	Velocity	Pipe D	Flow Rate	Mass Flow Ratio (%)
12oz Can	0.00582	0.015	1	0.14715	0.225209	4	1735.496	36.92545
Plastic Bag	0.05	0.0003884	1.4	0.00381	0.010449	4	80.52488	1.713295
Cigarette Butts	0.00024	0.00017	1	0.001668	0.118065	4	909.826	19.358
Snickers Wrapper	0.0123	0.00032	2	0.003139	0.016	4	123.2954	2.623307
Bottle Caps	0.007065	0.002	1.4	0.01962	0.063081	4	486.1098	10.34276
Straws	0.0012	0.0004	1	0.003924	0.080992	4	624.1355	13.27948
20oz pepsi bottle	0.0159	0.02383	1	0.233772	0.171738	4	1323.436	28.15821
16 oz Plastic Cup	0.006206	0.005	1	0.04905	0.125916	4	970.3281	20.64528
12oz glass bottle	0.01715	0.19	1	1.8639	0.466924	4	3598.191	76.55726

Type	Max Area	Mass	Cf	F	Velocity	Pipe D	Flow Rate	Mass Flow Ratio (%)
12oz Can	0.00582	0.015	1	0.14715	0.225209	3	976.2166	20.77057
Plastic Bag	0.05	0.0003884	1.4	0.00381	0.010449	3	45.29525	0.963729
Cigarette Butts	0.00024	0.00017	1	0.001668	0.118065	3	511.7771	10.88888
Snickers Wrapper	0.0123	0.00032	2	0.003139	0.016	3	69.35367	1.47561
Bottle Caps	0.007065	0.002	1.4	0.01962	0.063081	3	273.4368	5.817804
Straws	0.0012	0.0004	1	0.003924	0.080992	3	351.0762	7.469707
20oz pepsi bottle	0.0159	0.02383	1	0.233772	0.171738	3	744.4328	15.839
16 oz Plastic Cup	0.006206	0.005	1	0.04905	0.125916	3	545.8096	11.61297
12oz glass bottle	0.01715	0.19	1	1.8639	0.466924	3	2023.983	43.06346
Sand	0.00000078	0.0000044	1	4.32E-05	0.333182	3	1444.246	30.72863

A-2: Seaflo 4700GPH Pump Specifications [27]

STANDARD PUMP CONFIGURATIONS

Model	Flow Rate	Voltage	Max Draw	Fuse Amps	Head	Wire Lead	Outlet Dia	N.W. / G.W.
SFBP1-G4700-01	4451 GPH	12 V	32.1 A	26.0 A	26.2' (8 m)	3' (1 m)	2"	2.10/2.37 kg

PERFORMANCE

Voltage(V)	Current(A)	Flow		Head(M)
		GPH	LPH	
OPEN	14.6	4451	16844	0
12	16.2	4011	15179	1
12	18.5	3657	13839	2
12	20.1	2741	10373	3
12	22.6	1966	7440	4
12	25.2	831	3145	5
12	27.4	405	1533	6
12	30.9	136	515	7
12	32.1	0	0	8

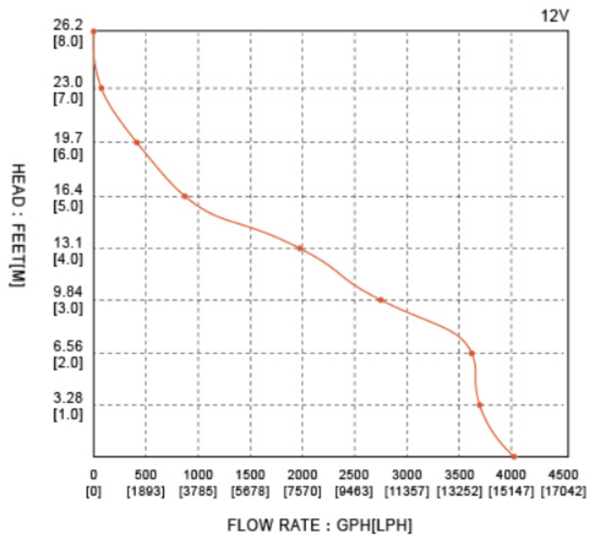

A-3: Sample 3D Printed Venturi Geometries

A-4: Flow Testing Data and Calculated Values

	length of tubing (ft)	height above ground (ft)	kg water	time		cu ft water	flow rate (cu ft/s)	Reynolds number	Darcy friction factor (estimate)	Darcy friction factor (recalculated)	flow rate (kg/s)	average flow rate (kg/s)	average flow rate (cu ft/s)	flow rate (ft/s)	frictional head loss (ft-lb/lb)	total head
Flexible hose	9	2	70.2	11.21		2.457	0.2191793042	108471.5472	0.01088764133	0.01904115361	6.262265834	6.026355771	0.210922452	1.116837219	0.01327668487	2.013276685
	9	2	70.2	11.57		2.457	0.2123595506	105096.4602	0.01088764133	0.01917646041	6.06741573			1.082086882	0.01255189639	2.012551896
	9	2	70.2	12.21		2.457	0.2012285012	99587.71861	0.01088764133	0.01941093368	5.749385749			1.025368159	0.01140834676	2.011408347
	9	4	67.8	13.77		2.373	0.1723311547	85286.4601	0.01088764133	0.02011520003	4.923747277	4.775563034	0.1671447062	0.8781205334	0.008670602049	4.008670602
	9	4	67.8	14.79		2.373	0.1604462475	79404.63526	0.01088764133	0.02045497752	4.584178499			0.8175604966	0.007642851786	4.007642852
	9	4	67.8	14.07		2.373	0.1686567164	83467.98547	0.01088764133	0.02021664801	4.818763326			0.8593972811	0.00834667943	4.008346679
	9	6	67.1	15.28		2.3485	0.153697644	76064.76034	0.01088764133	0.02066408063	4.391361257	4.047857787	0.1416750225	0.7831727082	0.007085129798	6.00708513
	9	6	67.1	17.08		2.3485	0.1375	68048.5678	0.01088764133	0.02122324491	3.928571429			0.7006369427	0.005823907716	6.005823908
	9	6	67.1	17.19		2.3485	0.136620128	67613.1203	0.01088764133	0.02125625603	3.903432228			0.6961535184	0.005758554091	6.005758554
	9	6	67.1	16.91		2.3485	0.1388823182	68732.67522	0.01088764133	0.02117197873	3.968066233			0.7076806021	0.005927242086	6.005927242
	5	2	65.3	10.75		2.2855	0.2126046512	105217.7601	0.01088764133	0.01917149232	6.074418605	6.028908202	0.2110117871	1.083335802	0.006987571101	2.006987571
	5	2	65.3	10.7		2.2855	0.2135981308	105709.4319	0.01088764133	0.01915143686	6.102803738			1.088398119	0.007045649856	2.00704565
	5	2	65.3	11.05		2.2855	0.2068325792	102361.1694	0.01088764133	0.01929067161	5.909502262			1.05392397	0.00665441743	2.006654417
	5	3.5	66.4	12.4		2.324	0.1874193548	92753.59036	0.01088764133	0.01972844315	5.35483871	5.439329871	0.1903765455	0.955003082	0.005587872515	3.505587873
	5	3.5	66.4	11.68		2.324	0.1989726027	98471.27744	0.01088764133	0.01946067963	5.684931507			1.013873135	0.006212542353	3.506212542
	5	3.5	66.4	12.58		2.324	0.1847376789	91426.43247	0.01088764133	0.01979392541	5.278219396			0.941338491	0.005447129395	3.505447129
Less flexible	9	2	60.1	11.24		2.1035	0.1871441281	92617.38102	0.01088764133	0.01973510304	5.346975089	5.131697328	0.1796094065	0.9536006528	0.01003203667	2.010032037
	9	2	60.1	12.14		2.1035	0.1732701812	85751.18308	0.01088764133	0.02008976044	4.950576606			0.882905382	0.008754265624	2.008754266
	9	2	60.1	11.79		2.1035	0.1784139101	88296.80769	0.01088764133	0.01995376509	5.097540288			0.9091154654	0.009218910108	2.00921891
	9	4	65.665	13.44		2.298275	0.1710026042	84628.96221	0.01088764133	0.02015152669	4.88578869	4.938036586	0.1728312805	0.8713508493	0.008552847041	4.008552847
	9	4	65.665	13.06		2.298275	0.1759781776	87091.36692	0.01088764133	0.02001746793	5.027947933			0.8967040899	0.008997546006	4.008997546
	9	4	65.665	13.4		2.298275	0.1715130597	84881.58597	0.01088764133	0.02013752254	4.900373134			0.8739518966	0.008598005752	4.008598006

A-5: Full Simulink Model for NiMH Battery Discharge